



# Molecular gut content analysis demonstrates that *Calanus* grazing on *Phaeocystis pouchetii* and *Skeletonema marinoi* is sensitive to bloom phase but not prey density

Jessica L. Ray<sup>1,\*</sup>, Katrine S. Skaar<sup>1</sup>, Paolo Simonelli<sup>2</sup>, Aud Larsen<sup>1</sup>, Andrey Sazhin<sup>3</sup>, Hans H. Jakobsen<sup>4</sup>, Jens C. Nejstgaard<sup>5</sup>, Christofer Troedsson<sup>1</sup>

<sup>1</sup>Uni Research Environment, Uni Research AS, Postboks 7810, 5020 Bergen, Norway

<sup>2</sup>Department of Biology, University of Bergen, 5020 Bergen, Norway

<sup>3</sup>P. P. Shirshov Institute of Oceanology, Russian Academy of Sciences, Laboratory of Ecology of Plankton Organisms, Nakhimovsky Prospect 36, Moscow, Russia

<sup>4</sup>Aarhus University, Bioscience, Frederiksborgvej 399, 4000 Roskilde, Denmark

<sup>5</sup>Leibniz Institute of Freshwater Ecology and Inland Fisheries, Dep. 3, Experimental Limnology, Alte Fischerhütte 2, 16775 Stechlin, Germany

**ABSTRACT:** Mesozooplankton grazing selection in complex marine microbial communities is a poorly understood yet critical structuring component of marine microbial food webs. We wished to quantitatively assess how relative grazing by the calanoid copepod *Calanus* spp. changed as a function of prey abundance dynamics in a controlled experimental setting. Our study focused on haptophyte- (*Phaeocystis pouchetii*) and diatom- (*Skeletonema marinoi*) dominated plankton communities in a 22 d seawater mesocosm experiment during the spring bloom in southwestern Norway. Using quantitative PCR, we analyzed the ratios of *P. pouchetii* or *S. marinoi* abundances in copepod gut content to their abundance in mesocosm seawater as proxies for understanding relative grazing across phytoplankton bloom development. We observed low relative grazing by *Calanus* on *P. pouchetii* and *S. marinoi* in mesocosms during peaks in phytoplankton abundance, suggesting that *Calanus* grazing on these phytoplankton was both low and uncoupled from phytoplankton density. We did observe a small but significant increase in relative grazing on *S. marinoi* after the demise of the diatom bloom, suggesting that senescent *S. marinoi* may be more bioavailable prey for *Calanus*. In conclusion, the use of qPCR ratios as proxy for relative prey consumption indicates the potential importance of phytoplankton bloom phase, but not relative prey density, for *Calanus* prey selection.

**KEY WORDS:** *Calanus* · Raunefjorden · qPCR · Copepod grazing · Mesocosm

## INTRODUCTION

Mesozooplankton, and in particular copepods (Maxillopoda: Copepoda), rank among the most abundant metazoans in the ocean, both in terms of abundance and biomass (Nejstgaard et al. 2008), according them

the substantial potential to influence the vertical flow of carbon and nutrients in the marine environment (Jónasdóttir et al. 2015). Copepods readily consume large diatom chains during seasons of upwelling and seasonal diatom blooms (Fessenden & Cowles 1994, Kjørboe & Nielsen 1994), thereby constituting a direct

\*Corresponding author: jessicalouiseray@gmail.com

link between primary production and higher trophic levels. Due to their small size, many phytoplankton species with diameters  $<5\ \mu\text{m}$  are not typically considered to be important food sources for copepods, which frequently exhibit prey choice based on size (Sommer et al. 2000) or swimming behavior (Kiørboe & Visser 1999), and even chemical cues in the case of larger aggregates (Goncalves & Kiørboe 2015). The high-latitude haptophyte *Phaeocystis* spp. has a unique life history in which it can alternate between single, flagellated cells of approx.  $4\ \mu\text{m}$  diameter, to large aggregates ('colonies') containing tens of thousands of non-motile cells (reviewed in Schoemann et al. 2005) during the spring bloom. This size variation raises the possibility that *Phaeocystis* colonies represent an abundant and important food source for copepods during the high-latitude spring bloom season.

There are conflicting reports on the role of *Phaeocystis* in the copepod diet (reviewed in Schoemann et al. 2005 and Nejstgaard et al. 2007). It has been argued that colony formation by *Phaeocystis* is a defense mechanism against grazing (Estep et al. 1990, Gasparini et al. 2000). Estep et al. (1990) investigated grazing by *C. finmarchicus* on natural microbial assemblages dominated by different physiological stages of a *P. pouchetii* bloom and observed that copepod consumption of *P. pouchetii* colonies in bottle incubation experiments occurred only when post-bloom colonies had begun to fragment. In another study of small copepods collected from the southern bight of the North Sea, Gasparini et al. (2000) were unable to detect grazing on *Phaeocystis* colonies when copepods were incubated with *P. globosa*-dominated natural microbial assemblages in bottle incubation experiments. The authors of those studies interpreted their findings as evidential of a life stage-specific defense behavior in the genus *Phaeocystis*, where colony formation is an anti-predation defense mechanism during bloom development (Jakobsen & Tang 2002, but see Irigoien et al. 2005), and that only during colony senescence does *Phaeocystis* become available as a food source for mesozooplankton. It remains unclear whether copepods contribute to top-down control of *Phaeocystis* blooms in high-latitude seas, or if this top-down control is dependent upon *Phaeocystis* bloom development.

Analysis of copepod gut content to identify feeding behavior *in situ* has often relied on pigment analysis (Gifford & Dagg 1988, Kleppel et al. 1991, Gasparini et al. 2000), but this method does not account for non-pigmented prey and is neither taxon-specific nor sensitive due to rapid degradation of pigments in the

copepod gut (Nejstgaard et al. 2008). Molecular detection of prey genomic DNA in the predator gut using quantitative PCR (qPCR) allows specific and rapid detection of any organism regardless of pigment content. The short DNA regions targeted by qPCR provide the ability to quantify prey despite partial DNA digestion in the predator gut (Nejstgaard et al. 2008, Durbin et al. 2008, Simonelli et al. 2009, Troedsson et al. 2009). One type of qPCR assay, the 5'-nuclease or 'TaqMan' assay (Gibson et al. 1996), provides an additional level of prey detection specificity through the inclusion of a probe that is highly specific for the target prey organism. Moreover, multi-copy gene targets, such as the small subunit ribosomal RNA (SSU rRNA) gene, increase the detectability of target prey organisms by providing many qPCR target sequences per prey cell. Studies using qPCR to quantify prey ingestion by copepods have traditionally used the SSU rRNA gene (Troedsson et al. 2007, Nejstgaard et al. 2008, Barofsky et al. 2010, Cleary et al. 2012, Durbin et al. 2012), although other multi-copy genes have also been targeted (e.g. mtCOI; Durbin et al. 2008).

Exploiting the sensitivity and specificity of TaqMan qPCR to investigate copepod feeding, our main objective was to determine whether grazing on *P. pouchetii* by *Calanus* copepods changes in response to *P. pouchetii* bloom development when this phytoplankton occurs in the context of natural mixed plankton assemblages in seawater mesocosms. For comparison, we also investigated *Calanus* grazing on different stages of bloom development of the diatom *Skeletonema* spp.

## MATERIALS AND METHODS

### Mesocosm experiment

A seawater mesocosm experiment was conducted at the Espegrend Marine Biological Station at the University of Bergen during 8–30 March 2012. Details of the mesocosm set-up are described elsewhere (Nejstgaard et al. 2006, Stoecker et al. 2015). Briefly, reinforced transparent polyurethane mesocosm bags were attached to floating mesocosm rings (Fig. 1A) and filled in a staggered mode on 8 March 2012 (Experimental Day 0) with  $11\ \text{m}^3$  water pumped from 5 m depth directly adjacent to the raft. Circulation of mesocosm water was achieved using an air lift system (Jacobsen et al. 1995). Two nutrient amendments were applied to triplicate mesocosm bags on 9 March (Experimental Day 1):  $16\ \mu\text{M}$  nitrate +  $1\ \mu\text{M}$  phos-

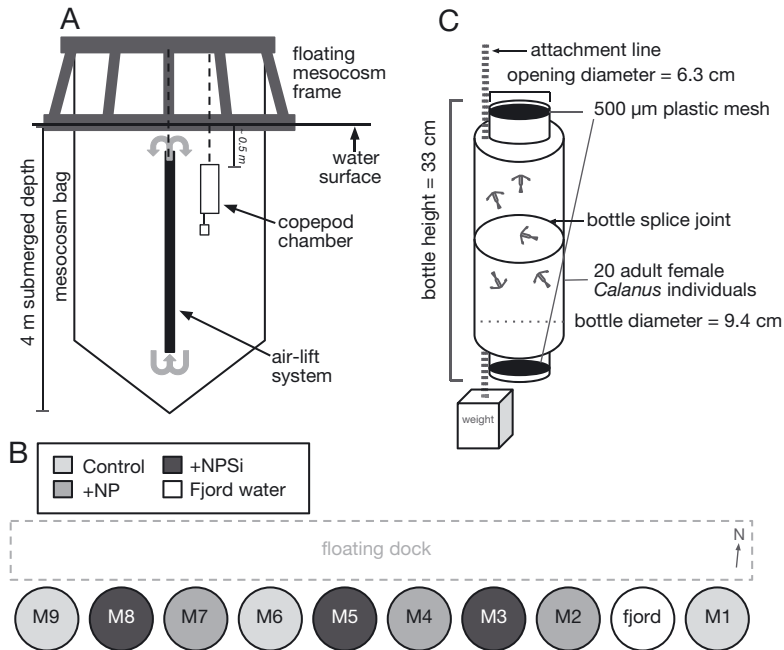


Fig. 1. Experimental setup and copepod chamber design and placement. (A) Schematic diagram of mesocosm bags in profile. (B) Mesocosm experimental set-up relative to raft orientation. Key shows treatments applied for individual mesocosm bags as denoted with 'M' and bag number; mesocosm frame labelled 'fjord' indicates the location of direct water sampling and copepod chamber placement in Raunefjorden. Treatment details are given in 'Materials and methods' and in Table 1. (C) Copepod chambers used for feeding experiments

plate (NP treatment,  $n = 3$ ) or  $16 \mu\text{M}$  nitrate +  $1 \mu\text{M}$  phosphate +  $5 \mu\text{M}$  silicate (NPSi treatment,  $n = 3$ ). Three mesocosm bags were unamended with mineral nutrients and served as experimental controls (Control treatment) for nutrient amendment (Fig. 1B). For reference, 1 set of samples was also taken from surface seawater directly adjacent to the mesocosm raft at the time of sampling from the mesocosm bags ('fjord' in Fig. 1B). Water samples from all 9 mesocosms and the adjacent fjord were collected daily for chlorophyll *a* (chl *a*) measurement as described in Holm-Hansen & Riemann (1978).

### Copepod chambers

Inspired by Barofsky et al. (2010), we designed flow-through copepod chambers to (1) contain copepods while (2) permitting free circulation of mesocosm water to allow copepods access to mesocosm microbiota and (3) facilitating rapid recovery and rinsing of copepods for molecular analysis. The chambers (Fig. 1C) were constructed by removing the bottom of two 1 l Nalgene bottles and wedging the open bottom of one bottle into the open bottom of the other

bottle until the 2 bottles overlapped by ca. 20 mm, thus creating a spliced container with a threaded opening at both ends. A 60 mm diameter hole saw was used to cut out the centers of the bottle lids. Nylon netting with  $500 \mu\text{m}$  mesh size was then secured over the bottle openings by sandwiching the mesh between the cut bottle lids and the bottle ends. Chambers were deployed in vertical orientation in mesocosms using strings attached to a bar across the mesocosm floating frames (Fig. 1A) and attaching weights (50 ml Falcon tube containing gravel) to the bottom opening of each chamber (Fig. 1C).

### Copepod collection and sorting

Mesozooplankton were collected from Raunefjorden ( $60^{\circ} 16' 18'' \text{N}$ ,  $5^{\circ} 10' 26'' \text{E}$ ) during March 2012 using a WP11 plankton net with  $100 \mu\text{m}$  mesh size and fitted with a cod end. Plankton nets were towed obliquely from 25 m to 10 m, then raised vertically from 10 m to surface, while vessel speed was maintained at 1 knot. Cod-end contents were gently diluted into buckets containing surface seawater (approx. temperature  $4\text{--}8^{\circ}\text{C}$ ) and kept in the shade during transport to land. Buckets containing collected mesozooplankton were kept at  $8^{\circ}\text{C}$  during sorting in the laboratory. Twenty active and physically undamaged individuals of adult *Calanus* spp. females (or CV juveniles when insufficient females were available) were pipette-sorted into each copepod chamber (Fig. 1C) standing in a 1 l beaker containing  $0.2 \mu\text{m}$ -filtered seawater ( $8^{\circ}\text{C}$ ). Chambers containing copepods were then closed with  $500 \mu\text{m}$  plastic mesh and incubated in the dark at  $8^{\circ}\text{C}$  overnight before being transferred to the mesocosms early the following day. Three replicate copepod chambers were mounted in each mesocosm approx. 0.5 m beneath the water surface (Fig. 1A).

### Seawater sampling

Seawater samples from mesocosms and Raunefjorden were collected daily between 07:00 and 08:00 h and kept at  $8^{\circ}\text{C}$  in the dark. Microscopy and Flow-CAM analysis were performed daily, while qPCR

analysis of seawater and mesocosm-incubated copepods was performed for samples collected on 11, 14, 17, 21, 24, 28 and 30 March 2012 only. The Control mesocosm M6 (Fig. 1B) developed a leak, and due to extensive volume loss was excluded from the sample collection after 21 March 2012.

### Microscopic and FlowCAM analysis of microeukaryotes in seawater

Sampling for microscopic analysis was performed daily for 1 mesocosm per treatment (M1, Control; M2, NP; and M3, NPSi) as described previously (Calbet et al. 2014). Additionally, *P. pouchetii*, *S. marinoi*, ciliates and the heterotrophic dinoflagellate *Gyrodinium cf. spirale* were counted daily in all mesocosms using a FlowCAM II (Fluid Imagine Technologies, Scarborough, ME). Detailed descriptions of microscopy and FlowCAM methods and instrument settings can be found in the Supplement at [www.int-res.com/articles/suppl/m542p063\\_supp.pdf](http://www.int-res.com/articles/suppl/m542p063_supp.pdf).

### Molecular analysis using qPCR

Seawater samples for qPCR analysis were collected from all mesocosms and Raunefjorden in separate once-rinsed 2 l bottles, and transported back to the laboratory for immediate filtration. Triplicate samples of 50–200 ml seawater were vacuum-filtered onto 25 mm diameter 0.2 µm pore size SUPOR filters (Pall). The volume of seawater used for filtration was reduced from 200 ml at the start of the experiment down to 50 ml in the NP and NPSi mesocosm treatments at the end of the experiment in order to reduce filter clogging by *P. pouchetii* colonies. However, this was corrected for in the analysis. Filters were transferred to 2.0 ml microcentrifuge tubes containing 280 µl 56°C ATL buffer (modified from the recommended 180 µl in the manufacturer's protocol) and 20 µl Proteinase K and tubes were inverted several times to coat filters completely with lysis solution. Filters were incubated at 56°C

Table 1. Summary of samples taken for molecular analysis during the seawater mesocosm experiment at the University of Bergen Marine Biological Station at Espeyrend in March 2012. Treatments — Control: seawater without nutrient amendment; +NP: seawater amended with 16 µM NO<sub>3</sub> and 1 µM PO<sub>4</sub>; +NPSi: seawater amended with 16 µM NO<sub>3</sub>, 1 µM PO<sub>4</sub> and 5 µM Si; none, water sampled from fjord surface directly adjacent to mesocosm raft, copepods incubated in surface water directly adjacent to raft. Volume filtered: volume of seawater filtered for molecular analysis, with 3 replicate filters per mesocosm per sampling day. No. of *Calanus*: number of adult female or CV *Calanus* individuals per mesocosm harvested for molecular gut content analysis

Sample ID	Date in March 2012	Experimental day	Mesocosms	Treatment	Volume filtered (ml)	No. of <i>Calanus</i>
Control11	11	3	M1, M6	Control	200	15
Control14	14	6	M1, M6, M9	Control	200	15
Control17	17	9	M1, M6, M9	Control	200	15
Control21	21	13	M1, M6, M9	Control	200	15
Control24	24	16	M1, M9	Control	200	15
Control28	28	20	M1, M9	Control	200, 100	15
Control30	30	22	M1, M9	Control	100, 50	15
NP11	11	3	M2, M4	+NP	200	15
NP14	14	6	M2, M4, M7	+NP	200	15
NP17	17	9	M2, M4, M7	+NP	200	15
NP21	21	13	M2, M4, M7	+NP	200	15
NP24	24	16	M2, M4, M7	+NP	200	15
NP28	28	20	M2, M4, M7	+NP	100	15
NP30	30	22	M2, M4, M7	+NP	50	15
NPSi11	11	3	M3, M5	+NPSi	200	15
NPSi14	14	6	M3, M5, M8	+NPSi	200	15
NPSi17	17	9	M3, M5, M8	+NPSi	200	15
NPSi21	21	13	M3, M5, M8	+NPSi	200	15
NPSi24	24	16	M3, M5, M8	+NPSi	200	15
NPSi28	28	20	M3, M5, M8	+NPSi	100	15
NPSi30	30	22	M3, M5, M8	+NPSi	100, 50, 50	15
Raunefjord11	11	3	Raft	None	200	15
Raunefjord14	14	6	Raft	None	200	15
Raunefjord17	17	9	Raft	None	200	15
Raunefjord21	21	13	Raft	None	200	15
Raunefjord24	24	16	Raft	None	200	15
Raunefjord28	28	20	Raft	None	100	15
Raunefjord30	30	22	Raft	None	50	15

overnight for lysis and protein digestion, then flash-frozen in liquid nitrogen and stored at –80°C. A summary of all samples taken for molecular analysis is given in Table 1.

After approximately 24 h incubations in mesocosms, copepod chambers were removed from mesocosms one at a time. Copepods collected on the bottom plastic mesh were rinsed by dipping chambers vertically into 3 consecutive 1 l beakers containing ultra-filtered seawater, prior to final immersion in anaesthetic seawater solution containing 0.37 mg ml<sup>-1</sup> ethyl 3-aminobenzoate methanesulfonate (MS222) (Sigma-Aldrich). Copepod recovery from mesocosm incubations commenced at the start of the day period (approx. 08:00 h) on sampling days, and copepod

sampling was always completed within 3 h after the start of sampling. Using a dissecting microscope and precision forceps, a pool of 5 copepod individuals was sorted from the anaesthetic solution into a 1.5 ml microcentrifuge tube containing 180  $\mu$ l of 56°C lysis buffer (Buffer ATL, QIAGEN DNeasy Blood & Tissue kit) and 20  $\mu$ l Proteinase K (QIAGEN kit, 20 mg ml<sup>-1</sup>). Samples were immediately mixed by inversion then placed in a 56°C heat block for tissue lysis and protein digestion overnight. Lysed samples were flash-frozen in liquid nitrogen and stored at -80°C until DNA extraction. Visual inspection of copepods upon recovery from mesocosm incubations confirmed that copepods had gut content and appeared to be healthy. Dead copepods, albeit rare, were occasionally recovered from chambers but were never sampled for molecular analysis.

#### DNA extraction

All DNA extractions were performed using the DNeasy Blood & Tissue kit (QIAGEN). Samples frozen in ATL buffer and Proteinase K were thawed on ice, heated briefly at 56°C, then vortexed for 2–3 s to re-dissolve precipitates in the lysis buffer. For seawater samples, filters were removed from tubes using a sterile pipette tip and discarded. Four microliters RNase A (20 mg ml<sup>-1</sup>, QIAGEN kit) was added to each sample, after which samples were incubated at room temperature (RT) for 2 min then vortexed vigorously for 15 s. After RNase digestion, 400  $\mu$ l of a 1:1 solution of AL buffer (QIAGEN kit) and 96% ethanol were added to all samples and mixed by vortexing. Binding of DNA to filter columns and sub-

sequent column washes were performed according to the manufacturer's protocol. Elution was performed with 2  $\times$  100  $\mu$ l 56°C Elution Buffer (QIAGEN kit). Samples were divided into 3 aliquots and stored at -20°C until analysis. This DNA extraction method was chosen based on previous studies demonstrating high DNA extraction efficiency and reproducibility using sample types similar to those collected in this study (Nejstgaard et al. 2008, Simonelli et al. 2009).

#### TaqMan detection of *Phaeocystis pouchetii* and *Skeletonema marinoi*

All primer and probe information can be found in Table 2. Primer and probe candidates (see Supplement) were tested for thermodynamic properties using the IDT OligoAnalyzer tool (<http://eu.idtdna.com/calc/analyzer>) and for target specificity using TestProbe and TestPrime on the Silva website ([www.arb-silva.de](http://www.arb-silva.de)). Primers Ppo-18S-Q-F1/Ppo-18S-Q-R1 amplify a 78 bp fragment in the V4 hypervariable region of the *P. pouchetii* SSU rRNA gene. The *P. pouchetii*-specific sense strand probe Ppo-q18S-probeC is located 4 nucleotides downstream of the Ppo-18S-Q-F1. The TaqMan assay for *S. marinoi* consists of primers Skel-175Fmod and Skel-244Rmod and the sense strand *S. marinoi*-specific probe KLEM-probeF located immediately downstream of the Skel-175F primer. This assay amplifies a 69 bp fragment in the V2 hypervariable region of the *S. marinoi*/*S. costatum* SSU rRNA gene. Both probes were dual-labelled with the fluorescent reporter dye 6-carboxyfluorescein (6-FAM) at their 5'-end and with the Black Hole Quencher-1 (BHQ1) at their 3'-end

Table 2. Primers and probes used in this study. 6-FAM: 6-carboxyfluorescein; BHQ1: Black Hole Quencher-1;  $T_{an}$ : annealing temperature used for qPCR; position: approximate nucleotide positions based on full-length eukaryotic SSU sequences for primers and probes designed in this study

Name	Sequence (5'–3')	Amplicon size (bp)	$T_{an}$ (°C)	Position	Reference
<b>Full-length eukaryotic SSU rRNA gene target for cloning</b>					
UnivF-15	CTGCCAGTAGTCATATGC	~1750	50	15–32	Frischer et al. (2000)
UnivR-1765S	ACCTTGTTACGACTT			1765–1751	Frischer et al. (2000)
<b><i>P. pouchetii</i>-specific V4 SSU rRNA for 5'-nuclease qPCR assay</b>					
18S-Ppo-Q-F1	ACTTTGAAAAAATCAGAGTG	78	56	776–795	This study
18S-Ppo-Q-R1	AGAGTCCTATTAATTATCCC			853–833	This study
Ppo-q18S-probeC	[6-FAM]CTAGCAGGCAGCTCGCTCTTG[BHQ1]			799–819	This study
<b><i>Skeletonema</i>-specific V2 SSU rRNA for 5'-nuclease qPCR assay</b>					
Skel-175Fmod	CCGCCGTGTTTATTAGTATT	69	55.8	175–194	Barofsky et al. (2010)
Skel-244Rmod	CAATTCGAAAGGTTATTATGACT			244–222	Barofsky et al. (2010)
KLEM-probeF	[6-FAM]AAACCTTCACTCTTCGGAGTTGATTTG[BHQ1]			195–211	This study

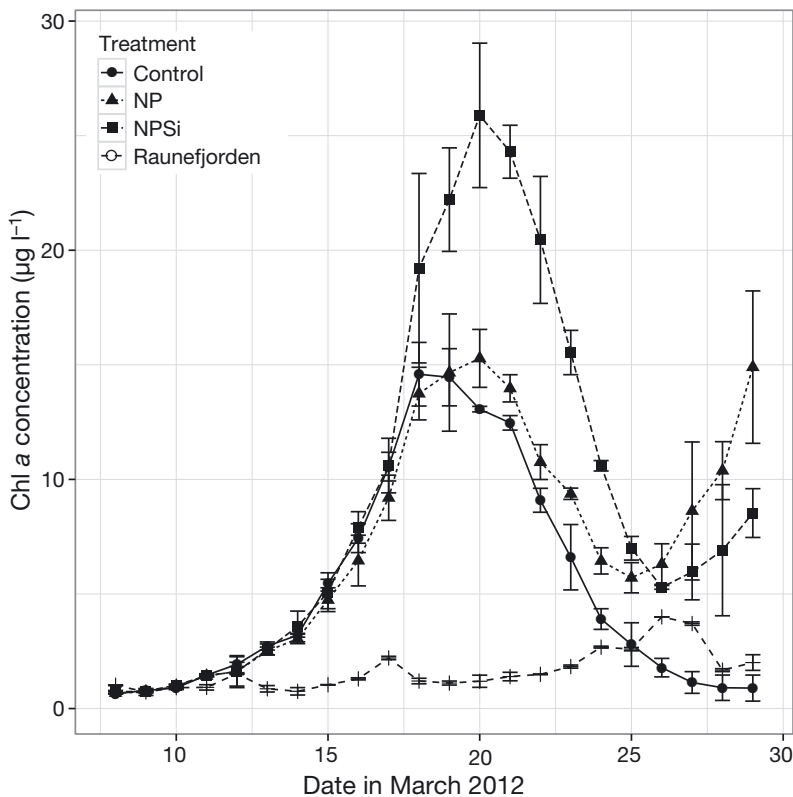


Fig. 2. Chlorophyll a concentration in all mesocosm bags and the adjacent Raunefjorden. Error bars show 95% confidence intervals for triplicate measurements.

and were purchased HPLC-purified from Sigma-Aldrich. Assays were run on a CFX96 Real-Time System (Bio-Rad) in 20  $\mu$ l reactions prepared with SsoFast (*P. pouchetii*) or SsoAdvanced (*S. marinoi*) Universal Probes Supermix (Bio-Rad). *P. pouchetii* detection reactions contained 1 $\times$  supermix, 900 nM each primer, 250 nM probe, and 4  $\mu$ l template and were run with the program 98 $^{\circ}$ C for 2 min, then 40 cycles of 95 $^{\circ}$ C for 10 s and 56 $^{\circ}$ C for 5 s, followed by plate read. *S. marinoi* qPCR reactions contained 1 $\times$  supermix, 250 nM of each primer and probe and 4  $\mu$ l template and were run with the program 95 $^{\circ}$ C for 3 min, then 40 cycles of 95 $^{\circ}$ C for 10 s and 55.8 $^{\circ}$ C for 10 s, followed by plate read. qPCR results for *P. pouchetii* or *S. marinoi* SSU rRNA were normalized to gene copies copepod<sup>-1</sup> or gene copies ml<sup>-1</sup> for copepod gut content and seawater samples, respectively.

### Statistical analysis

All statistical analyses and data visualizations were conducted using the R statistical computing environment (R Core Team 2015). qPCR results of cycle

threshold ( $C_T$ ) values >40 cycles (i.e. not detected) for *P. pouchetii* and *S. marinoi* in some copepod samples were manually changed to SSU rRNA gene copy number = 1 in order to allow inclusion of these data points in statistical calculations. Ratios from qPCR analysis (ratio = gene copies copepod<sup>-1</sup> / gene copies ml<sup>-1</sup>) were tested for significant changes over time using the `posthoc.kruskal.nemenyi.test` function in the `PMCMR` package (Pohlert 2015). The R packages `base` and `ggplot2` (Wickham 2009) were used for data visualization.

## RESULTS

### Chlorophyll a dynamics

Chl a measurements (Fig. 2) indicated that 2 phytoplankton blooms occurred during the mesocosm experiment. The first bloom, or exponential increase in phytoplankton growth, was delimited by a chl a maximum on 19–21 March in all 3 mesocosm treatments (Control, NP and NPSi). During this bloom period, a chl a maximum of 25  $\mu$ g chl a l<sup>-1</sup> was observed in the NPSi treatment, while peak chl a concentrations in the NP and Control mesocosm treatments were approx. 15  $\mu$ g l<sup>-1</sup>. A subsequent phytoplankton bloom became evident as a second chl a increase on 28–30 March in the NP and NPSi mesocosm treatments. This second bloom period reached chl a concentrations of 12  $\mu$ g l<sup>-1</sup> in the NP treatment and 6  $\mu$ g l<sup>-1</sup> in the NPSi treatment. Chl a concentrations in Raunefjorden were always  $\leq$  3  $\mu$ g l<sup>-1</sup>, although 2 weak increases in chl a were observed on 17 March and on 26–27 March (Fig. 2, open symbols).

### Quantification of *Phaeocystis pouchetii* in seawater

Microscopy (Fig. 3A) and FlowCAM (Fig. 3B) analysis of mesocosm seawater confirmed that the increasing chl a concentration toward the end of the mesocosm experiment (Fig. 2) was due to *P. pouchetii* blooms in the NP and NPSi mesocosm treatments. The strongest *P. pouchetii* increase was observed in the NP treatment, with peak abundances of approx. 10<sup>5</sup> cells ml<sup>-1</sup> as measured by both microscopy and

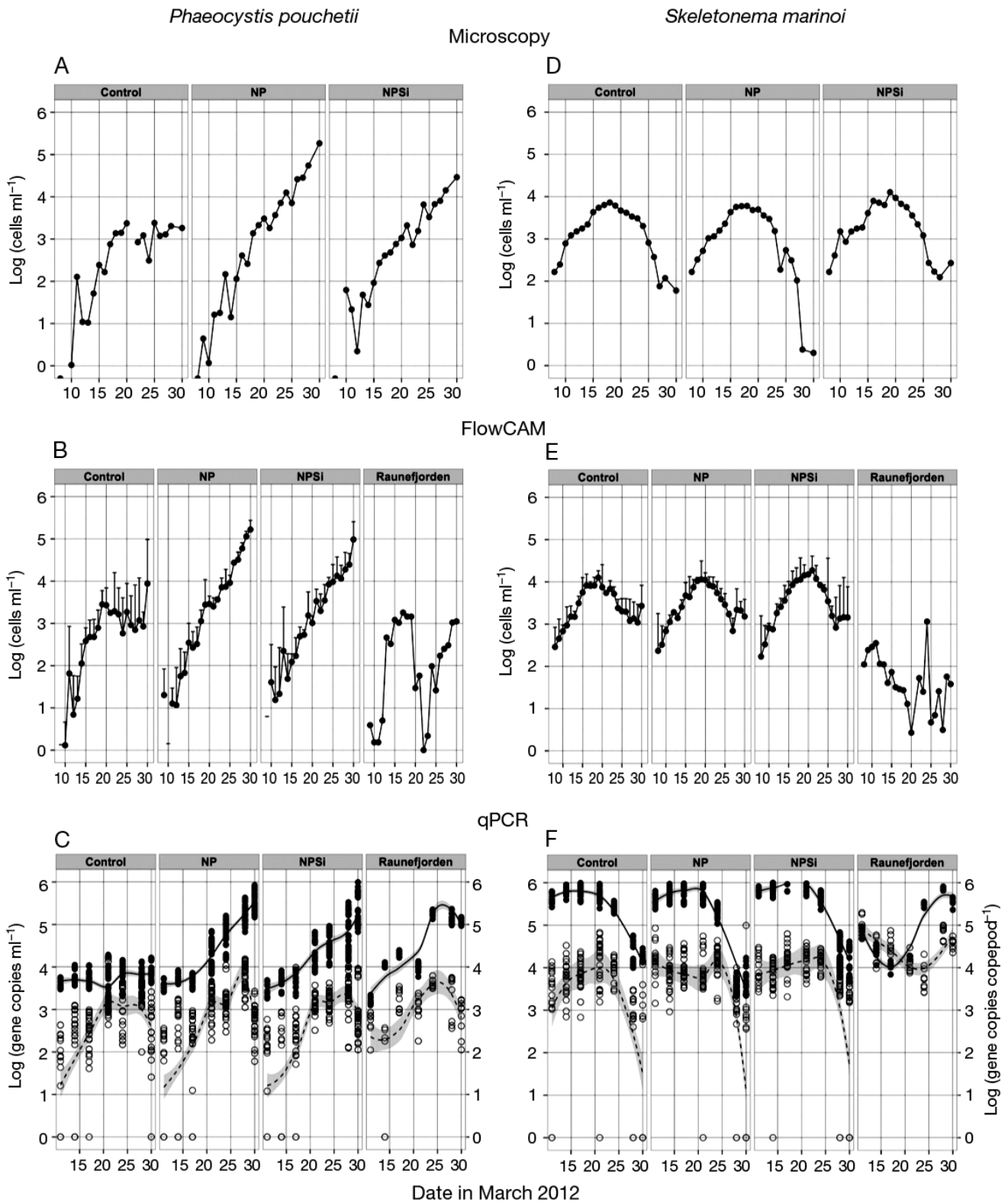


Fig. 3. Quantification results for (A–C) *Phaeocystis pouchetii* and (D–F) *Skeletonema marinoi* during March 2012. The y-axis units for qPCR results (C,F) are gene copies  $\text{ml}^{-1}$  (black circles and solid trendline) or gene copies copepod $^{-1}$  (open circles and dashed trendline). Error bars for (B,E) show standard deviation from the mean ( $n = 2$  or 3 replicates). Trendlines for (C,F) were calculated using the loess smoothing function, with grey zones indicating 95% confidence intervals

FlowCAM analysis (Fig. 3A,B). *P. pouchetii* comprised >80 % of microeukaryotes present in the NP samples at the time of peak abundance (Fig. S1A in the Supplement). Slightly lower *P. pouchetii* peak density (Fig. 3A,B) and relative abundance (Fig. S1A) were observed in the NPSi mesocosm treatment, with observed peak densities of  $\sim 2 \times 10^4$  cells ml<sup>-1</sup> by microscopy (Fig. 3A) or  $\sim 10^5$  cells ml<sup>-1</sup> by FlowCAM (Fig. 3B) measurement. For the Control mesocosms, both microscopy (Fig. 3A) and FlowCAM analysis (Fig. 3B) detected an increase in colonial *P. pouchetii* cells from 9 March until 20 March, at which time the *P. pouchetii* abundance stabilized at approx.  $10^3$  cells ml<sup>-1</sup>. This low *P. pouchetii* abundance plateau in Control mesocosms is in accord with stably low chl *a* concentration in these mesocosms during the latter half of the experiment (Fig. 2). Comparison of *P. pouchetii* qPCR results with microscopy or FlowCAM counts for *P. pouchetii* cells shows linear relationships between microscopic and molecular methods, with variable degrees of fit (Fig. S2 in the Supplement).

*P. pouchetii* abundance in seawater as measured by qPCR was determined to be  $\sim 5 \times 10^3$  copies ml<sup>-1</sup> on 11 March for all treatments and Raunefjorden (Fig. 3C). Thereafter, *P. pouchetii* target gene copies in seawater increased exponentially in the NP and NPSi mesocosm treatments after 17 March, and after 21 March in Raunefjorden (Fig. 3C). *P. pouchetii* target gene copies peaked at approx.  $1\text{--}2 \times 10^5$  copies ml<sup>-1</sup> on 30 March in the NP and NPSi mesocosm treatments (Fig. 3C), while in Raunefjorden the target gene copy number peaked at  $10^5$  copies ml<sup>-1</sup> on 24 March (Fig. 3C). The Control was characterized by stable *P. pouchetii* target gene counts of approximately  $5 \times 10^3$  gene copies ml<sup>-1</sup> throughout the experimental period (Fig. 3C), in contrast to the approx. 100-fold increases in cell counts as measured by microscopy (Fig. 3A) or FlowCAM (Fig. 3B). In the NP and NPSi mesocosm treatments, peak *P. pouchetii* target gene copy abundances (Fig. 3C) in general corresponded to peak cell abundances measured by microscopy (Fig. 3A) and FlowCAM (Fig. 3B), whereas in the Control they were slightly higher than peak cell abundances determined by microscopy (Fig. 3A). FlowCAM analysis of seawater from Raunefjorden (Fig. 3B) showed a bimodal growth dynamic for *P. pouchetii* characterized by 2 apparent growth peaks interspersed by a sharp decline, although qPCR analysis of Raunefjorden seawater indicated an increase in *P. pouchetii* target gene copies up to 24 March when numbers stabilized (Fig. 3C).

### Quantification of *Skeletonema marinoi* in seawater

Microscopy (Fig. 3D) and FlowCAM analysis (Fig. 3E) over the course of the experiment confirmed that the first peaks in chl *a* observed around 19–21 March in the Control, NP and NPSi mesocosm treatments (Fig. 2) was attributed to the chain-forming diatom *S. marinoi*. At peak abundance, *S. marinoi* reached densities of approx  $10^4$  cells ml<sup>-1</sup> (Fig. 3D) and accounted for 35–50% of the total microeukaryote abundance as determined by microscopy (Fig. S1B). FlowCAM analysis identified similar trends in *S. marinoi* abundance when *S. marinoi* quantification results from all mesocosms for each treatment were averaged (Fig. 3E), demonstrating reproducible trends in *S. marinoi* dynamics in replicate mesocosms. *S. marinoi* in the adjacent Raunefjorden occurred at densities of  $10^1$  to  $10^2$  cells ml<sup>-1</sup> during the experimental period, but with no clear indication of bloom-like exponential growth. FlowCAM counts from Raunefjorden show general low abundances of *S. marinoi* and confirmed that no *S. marinoi* bloom development occurred at any time during the experiment.

Using qPCR to quantify *S. marinoi* in seawater (Fig. 3F), we observed slightly different trends in *S. marinoi* growth in mesocosms when compared with growth dynamics measured using microscopy (Fig. 3D) or FlowCAM (Fig. 3E) analysis. Specifically, qPCR demonstrated that *S. marinoi* in the NPSi mesocosm treatment peaked at approx.  $10^6$  target gene copies ml<sup>-1</sup> (Fig. 3F), whereas peak cell abundances of *S. marinoi* measured by microscopy (Fig. 3D) or FlowCAM analysis (Fig. 3E) were about  $10^4$  cells ml<sup>-1</sup> in the NPSi treatment. This relative quantification difference (Fig. S2), which is apparent for all 3 mesocosm treatments, is likely due to the multicopy nature of the *S. marinoi* SSU rRNA gene locus, which is present in approximately 70 copies per cellular genome (A.-L. Godhe, Univ. of Gothenburg, pers. comm.). Microscopy and FlowCAM analysis, in contrast, quantify individual cells. Incidentally, we did not observe a similar magnitude discrepancy in *P. pouchetii* target gene abundances from qPCR analysis with *P. pouchetii* cellular abundances as measured by microscopy and FlowCAM analysis (Fig. 3A–C). *S. marinoi* abundances in the Control, NP and NPSi mesocosms peaked at just under  $10^6$  target gene copies ml<sup>-1</sup> on 21 March, then decreased rapidly to approx.  $10^4$  gene copies ml<sup>-1</sup> by 30 March (Fig. 3), at which abundance they remained until the end of the experiment. All 3 quantification methods



showed that the highest peak in *S. marinoi* abundance occurred in the NPSi mesocosm treatment (Fig. 3D–F). In Raunefjorden, qPCR detection of *S. marinoi* identified an initial decline in *S. marinoi* target gene copies, from  $5 \times 10^4$  gene copies  $\text{ml}^{-1}$  on 11 March to  $1 \times 10^4$  gene copies  $\text{ml}^{-1}$  on 17 March (Fig. 3F). After 17 March, however, *S. marinoi* gene copy numbers in Raunefjorden increased to over  $10^5$  gene copies  $\text{ml}^{-1}$  by the end of the experiment. The dynamic ranges of *S. marinoi* in Raunefjorden as measured by FlowCAM (Fig. 3E) or qPCR (Fig. 3F) were similarly compact (approximately one order of magnitude), which would corroborate chl *a* measurements (Fig. 2) showing no large increases in autotroph (phytoplankton) growth during the experimental period.

### Copepod gut content analysis

qPCR analysis of copepod samples revealed a trend of increasing *P. pouchetii* target gene copies in the copepod gut in the Control, NP and NPSi mesocosm treatments, with copy numbers ranging from approx 100–500 copies copepod<sup>-1</sup> on 11 March to  $1\text{--}2 \times 10^3$  copies copepod<sup>-1</sup> on 28 March (Fig. 3C). In samples from copepods that had been incubated in Raunefjorden, we observed an initial increase in *P. pouchetii*, from ~200 gene copies copepod<sup>-1</sup> on 11 March to  $\sim 5 \times 10^3$  gene copies copepod<sup>-1</sup> on 24 March (Fig. 3C). Subsequently, *P. pouchetii* in Raunefjorden-incubated copepods decreased to ~500 gene copies copepod<sup>-1</sup> by 30 March. From qPCR analysis of *S. marinoi* in copepod samples (Fig. 3F), we observed different trends in *S. marinoi* signals over time. In the Control, the number of *S. marinoi* target gene copies started at  $\sim 10^3$  copies copepod<sup>-1</sup> on 11 March, increased to  $\sim 10^4$  copies copepod<sup>-1</sup> around the time of the *S. marinoi* bloom peak around 21 March, then decreased until the end of the experiment. For copepods incubated overnight in the NP and NPSi mesocosms, however, we observed higher initial *S. marinoi* target gene copy numbers, approx.  $10^3$  copies copepod<sup>-1</sup>, until 24 March, after which *S. marinoi* signal in copepod samples decreased similar to the Control (Fig. 3F). For Raunefjorden copepod samples, we observed an initial decline in target gene copy numbers from approx.  $10^5$  copepod<sup>-1</sup> on 11 March to  $10^4$  copepod<sup>-1</sup> on 24 March. After 24 March, *S. marinoi* qPCR signal in Raunefjorden copepod samples increased to approx.  $3 \times 10^4$  copepod<sup>-1</sup> (Fig. 3F).

### qPCR ratios as proxies for relative grazing by *Calanus*

In order to obtain a measure for grazing activity by *Calanus* on either *P. pouchetii* (Fig. 4A) or *S. marinoi* (Fig. 4B) relative to specific phytoplankton densities in seawater, we calculated the pairwise ratios of individual qPCR signals in copepod samples (normalized to copies copepod<sup>-1</sup>) to individual qPCR signals in seawater (normalized to copies  $\text{ml}^{-1}$ ) at the time of recovery of copepods from overnight mesocosm incubations. Individual mesocosm treatments and Raunefjorden were tested for a significant effect on sampling date on qPCR ratios using Kruskal-Wallis tests. For *P. pouchetii*, we observed a significant increase in qPCR ratios over time in the Control (Table 3), while qPCR ratios in the NP and NPSi mesocosm treatments, in which *P. pouchetii* blooms occurred near the end of the experimental period, decreased significantly across the experimental period. qPCR ratios also decreased significantly over time in Raunefjorden samples (Fig. 4A, Table 3). Kruskal-Wallis tests of *S. marinoi* qPCR ratios, in contrast, identified significant increases over time in the Control, NP and NPSi mesocosm treatments (Fig. 4B, Table 3), while a significant decrease in *S. marinoi* qPCR ratios was observed in Raunefjorden samples (Fig. 4B and Table 3). The strongest temporal difference in *S. marinoi* qPCR ratios occurred between 21 March and 28 March in the NP ( $p < 0.0001$ ) and NPSi ( $p = 0.00046$ ) mesocosms. The increasing trend in *S. marinoi* qPCR ratios in mesocosms over time (Fig. 4B) was coincident with the decline of the *S. marinoi* bloom in these treatments (Fig. 3D–F). For Raunefjorden samples, higher *S. marinoi* ratios were observed during the first half of the experiment, but these dropped sharply after 21 March ( $p = 0.00616$ ), coincident with an apparent recovery of *S. marinoi* populations in Raunefjorden at this time (Fig. 3D–F).

## DISCUSSION

One of the main purposes of this study was to test whether relative grazing by *Calanus* on *P. pouchetii* changes in response to *P. pouchetii* bloom development in natural assemblages of phyto- and microplankton. Our qPCR results suggest that neither single-celled nor colonial *P. pouchetii* cells contributed significantly to *Calanus* diet, not even when *P. pouchetii* reached high abundances at the end of the experiment. As a consequence of incomplete *P. pou-*

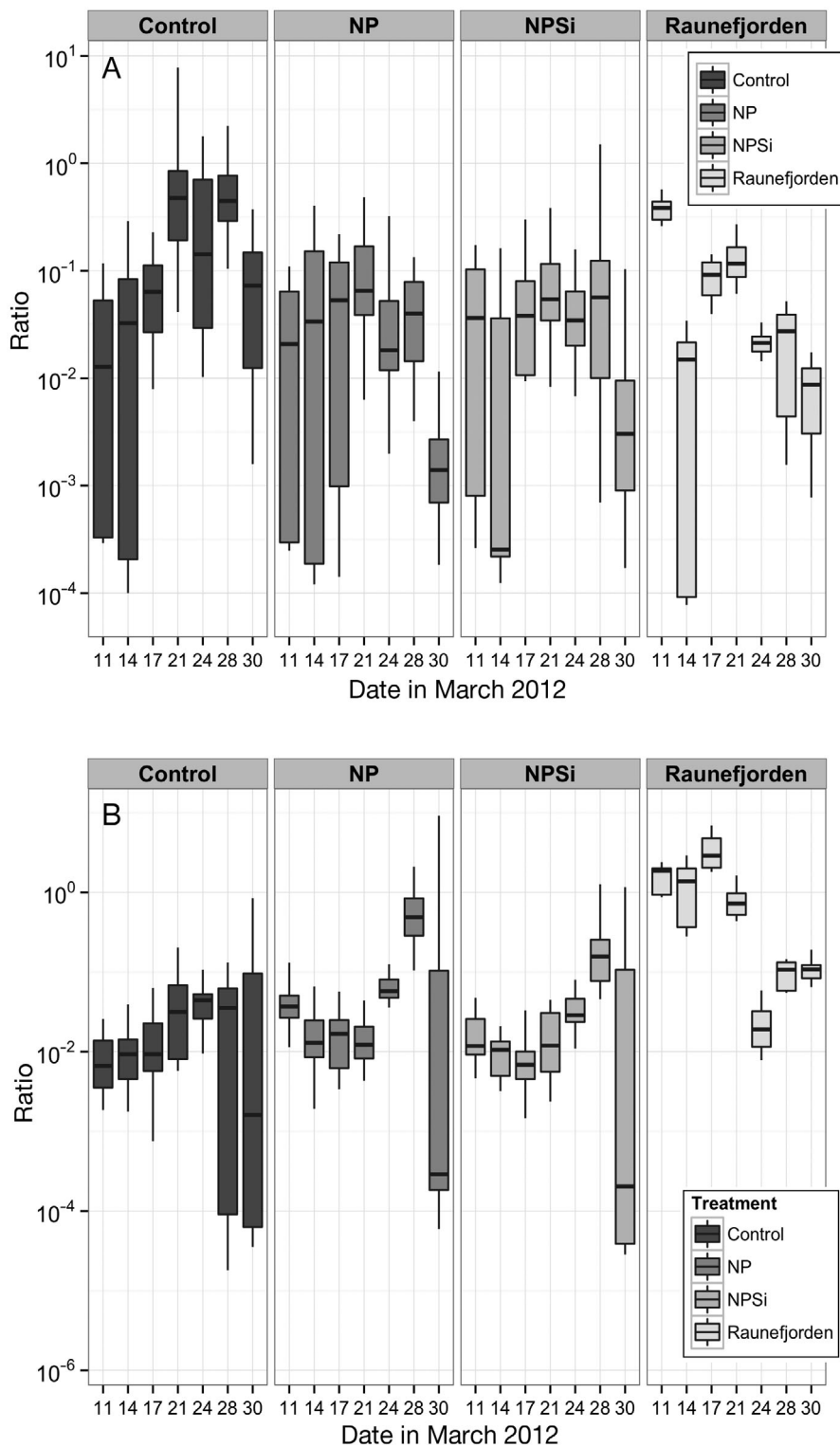


Fig. 4. Box-and-whisker plots showing qPCR target gene copy number ratios for (A) *Phaeocystis pouchetii* or (B) *Skeletonema marinoi* in the gut content of copepods (copies copepod<sup>-1</sup>) relative to gene copy abundance in seawater (copies ml<sup>-1</sup>). Line: median; box: 25th–75th percentiles; whiskers: 5th–95th percentiles; outliers not shown for simplicity

*chetii* bloom development, however, we were unable to assess the soundness of the hypothesis that colony formation by *P. pouchetii* serves to inhibit predation by *Calanus* copepods (Estep et al. 1990). Production of DMSP, acrylic acid and extracellular polysaccharides (Dutz et al. 2005 but see also Huntley et al. 1987, Kuhlisch & Pohnert 2015) by *Phaeocystis* may have increased avoidance by copepods, however the influence of chemical factors on *Calanus* grazing has not been tested here.

Our grazing proxy also allowed us to identify an inverse relationship between *S. marinoi* bloom development and increased consumption of *S. marinoi* by *Calanus* toward the end of the experiment. This is similar to a report by (Barofsky et al. 2010), suggesting that dead or dying *S. marinoi* cells may be more bioavailable for *Calanus*. While inside mesocosm chambers, copepods had access to abundant and diverse prey organisms of potentially higher nutritional quality, including ciliates and dinoflagellates (Gifford & Dagg 1988, Kleppel et al. 1991), allowing copepods to be selective in their choice of prey (e.g. Kleppel 1993, Kjørboe et al. 1996, Leising et al. 2005a, and references below). Although our qPCR ratios indicate that *S. marinoi* bloom declines were positively correlated with increased relative consumption by copepods (Fig. 4B), there is also the possibility that *S. marinoi* in mesocosm decreased due to grazing by microzooplankton. We also observed an increase in the dinoflagellate *Gyrodinium spirale* in all mesocosm treatments (Control, NP and NPSi) over the course of the experiment (Fig. S3B in the Supplement), which may offer an alternative explanation for the decline in abundance of *S. marinoi* in mesocosm treatments after 24 March (Fig. 3E–G). This heterotrophic dinoflagellate is specialized in grazing on chain-forming

Table 3. Influence of sampling date on qPCR ratios for each treatment as determined by Kruskal-Wallis pairwise comparisons using Tukey and Kramer (Nemenyi) posthoc tests for independent interactions. Significant results ( $\alpha = 0.05$ ) are in **bold**

Date	<i>Phaeocystis pouchetii</i>						<i>Skeletonema marinoi</i>						
	March	11	14	17	21	24	28	11	14	17	21	24	28
<b>Control</b>													
14	0.99891	–	–	–	–	–	–	0.9881	–	–	–	–	–
17	0.65156	0.85839	–	–	–	–	–	0.9343	0.9999	–	–	–	–
21	<b>1.9e-09</b>	<b>1.7e-10</b>	<b>1.8e-06</b>	–	–	–	–	<b>0.0158</b>	0.0654	0.1581	–	–	–
24	<b>0.00098</b>	<b>0.00120</b>	0.11654	0.08597	–	–	–	<b>0.0016</b>	<b>0.0073</b>	<b>0.0214</b>	0.9569	–	–
28	<b>9.8e-09</b>	<b>2.0e-09</b>	<b>7.2e-06</b>	1.00000	0.10809	–	–	0.3669	0.7402	0.8964	0.9438	0.5110	–
30	0.58030	0.80523	1.00000	<b>1.1e-07</b>	0.07118	<b>8.7e-07</b>	–	0.7050	0.9647	0.9957	0.6797	0.2132	0.9987
<b>NP</b>													
14	0.99398	–	–	–	–	–	–	0.22246	–	–	–	–	–
17	0.63640	0.92447	–	–	–	–	–	0.22893	1.00000	–	–	–	–
21	<b>0.00125</b>	<b>0.00341</b>	0.17395	–	–	–	–	0.11162	0.99988	0.99984	–	–	–
24	0.78260	0.98629	0.99889	<b>0.00540</b>	–	–	–	0.89058	<b>0.00137</b>	<b>0.00146</b>	<b>0.00032</b>	–	–
28	0.23643	0.54609	0.99861	0.20741	0.87673	–	–	0.09237	<b>3.0e-07</b>	<b>3.3e-07</b>	<b>4.0e-08</b>	0.62121	–
30	0.07345	<b>0.00076</b>	<b>1.4e-06</b>	<b>5.2e-14</b>	<b>4.0e-08</b>	<b>8.9e-12</b>	–	0.04490	0.99171	0.99069	0.99978	<b>5.6e-05</b>	<b>3.6e-09</b>
<b>NPSi</b>													
14	0.09001	–	–	–	–	–	–	0.75565	–	–	–	–	–
17	1.00000	<b>0.02709</b>	–	–	–	–	–	0.61331	0.99998	–	–	–	–
21	0.37904	<b>7.4e-08</b>	0.26161	–	–	–	–	0.99951	0.90360	0.78935	–	–	–
24	0.99384	<b>0.00033</b>	0.99411	0.44680	–	–	–	0.41407	<b>0.00190</b>	<b>0.00068</b>	0.09356	–	–
28	0.89623	<b>1.9e-05</b>	0.86585	0.88754	0.99060	–	–	<b>0.01406</b>	<b>1.3e-06</b>	<b>3.3e-07</b>	<b>0.00046</b>	0.73766	–
30	<b>0.03163</b>	1.00000	<b>0.00417</b>	<b>6.3e-12</b>	<b>1.9e-06</b>	<b>2.6e-08</b>	–	0.99995	0.83578	0.69356	1.00000	0.13864	<b>0.00092</b>
<b>Raunefjorden</b>													
14	<b>1.8e-05</b>	–	–	–	–	–	–	0.99969	–	–	–	–	–
17	0.81772	<b>0.00698</b>	–	–	–	–	–	0.91853	0.72662	–	–	–	–
21	0.79047	<b>0.00040</b>	1.00000	–	–	–	–	0.90543	0.98763	0.24299	–	–	–
24	<b>0.00045</b>	0.77719	0.10917	<b>0.00999</b>	–	–	–	<b>4.0e-05</b>	<b>0.00026</b>	<b>8.1e-08</b>	<b>0.00616</b>	–	–
28	<b>0.00020</b>	0.86795	0.06817	<b>0.00449</b>	0.99999	–	–	<b>0.01585</b>	0.05439	<b>0.00017</b>	0.32475	0.77995	–
30	<b>6.4e-09</b>	0.99649	<b>5.0e-05</b>	<b>4.9e-08</b>	0.15258	0.24486	–	<b>0.02411</b>	0.07753	<b>0.00031</b>	0.40256	0.70245	1.00000

diatoms such as *S. marinoi* (Stelfox-Widdicombe et al. 2004, Sherr & Sherr 2007).

According to both models and empirical data, mesozooplankton such as *Calanus* are more likely to graze on ciliates and large diatoms than on microalgae such as *P. pouchetii* (Nejstgaard et al. 1997, 2001, Irigoien et al. 2005, Thingstad et al. 2008). Protistan microzooplankton comprise a significant fraction of mesozooplankton diet (Stoecker & Capuzzo 1990), and in certain cases can be preferred prey species as assessed by clearance rate measurements in the laboratory (Hansen 1995, Gasparini et al. 2000) and in field studies (Kleppel et al. 1991, Leising et al. 2005b, Huo et al. 2008). This may in part be due to the higher nutritional value of microzooplankton (reviewed in Stoecker & Capuzzo 1990, but see Koski et al. 2005, Huo et al. 2008) and/or to greater conspicuousness of ciliates caused by their larger size and higher motility (Jakobsen et al. 2005) relative to

*Phaeocystis* cells (Klein Breteler & Koski 2003, Koski et al. 2005 and references therein). Indeed, ciliates were present in all mesocosm treatments over the experimental period (Fig. S3A). The spike in ciliate abundance in Raunefjorden on 12 March in combination with qPCR ratios showing *Calanus* grazing on *P. pouchetii* after 15 March indicate that *Calanus* may have consumed ciliates rather than *P. pouchetii* from 12–14 March. Once ciliates were grazed down to low abundances observed on 15 March, *Calanus* consumed *P. pouchetii* (Jonsson & Tiselius 1990), albeit at low levels (Fig. 3C).

In some copepod samples we were unable to detect *P. pouchetii* or *S. marinoi*. We believe the most probable explanation for the lack of qPCR signals is genuinely low rates of ingestion of *P. pouchetii* or *S. marinoi*, as discussed above. We cannot, however, rule out temporal variability in copepod grazing, or technical factors associated

with prey detection. The sensitivity of the TaqMan assays used in this study (linear detection as low as 100 target gene copies) suggest that even a very few cells should be detectable given the multi-copy nature of the target SSU rRNA genes. Alternatively, copepod digestion rates might have changed across the course of the experiment, altering prey detectability independent of actual ingestion rates (Mayzaud & Razouls 1992). Since copepods were allowed 24 h to acclimate to the mesocosm environment prior to sampling, we find no reason to believe this to be the case in our experiment. Prey DNA degradation in the copepod gut was not corrected for in this study (Simonelli et al. 2009, Troedsson et al. 2009), and little is known about the relative rates of digestion of different phytoplankton prey particles after ingestion by predators. The silicate frustule of *S. marinoi* may protect it from rapid digestion during gut passage (Peterson & Jones 2003) in copepods, while *P. pouchetii* cells possess no hard external structures and may therefore be digested at a faster rate. One comparative study of digestion rates, assessed as rate of visual disappearance, of whole ciliates and dinoflagellate cells fed to the ctenophore *Mnemiopsis leidyi* showed that naked ciliate and dinoflagellate taxa were digested much faster than loricate or thecate taxa (Sullivan 2010). However, Troedsson et al. (2009) demonstrated qPCR detection of a 74 bp prey DNA fragment up to 30 min after prey consumption by *Calanus* copepods in the laboratory, suggesting that cellular lysis of prey in the predator gut is temporally uncoupled from prey DNA degradation.

We chose to use copepod chambers, rather than direct collection, for incubation and recovery of *Calanus* copepods in mesocosms (or Raunefjorden) prior to gut content analysis by qPCR, mainly because such net sampling intensity in the mesocosms would have jeopardized the entire experiment. The size of the mesh (500  $\mu\text{m}$ ) covering the openings of the chambers was chosen as the best trade-off between the free passage of the natural diversity of prey organisms through copepod chambers and our ability to safely contain and recover *Calanus* copepods. Undamaged and active *Calanus* individuals were exclusively chosen for chamber incubations, and full gut content was visually assessed during sorting upon copepod recovery from chambers (P. Simonelli pers. obs.), allaying concerns that copepods were not feeding during the incubation period. The low and zero qPCR results for *P. pouchetii* and *S. marinoi* in copepod samples thus likely represent

genuinely low rates of ingestion of these prey organisms. However, the large size of *P. pouchetii* colonies (up to several millimeters in diameter) in the NP and NPSi mesocosms on the last sampling day of the experiment (30 March) may have prevented passage through the plastic mesh, making *P. pouchetii* and possibly *S. marinoi* less available as food particles. Due to the potential technical bias associated with the 30 March samples, qPCR results for the NP and NPSi treatments on this date should be interpreted with caution. Full assessment of *Calanus* feeding selection and prey preference during *P. pouchetii* or *S. marinoi* blooms would require information about all prey particles ingested, however this falls outside the scope of this study.

Our qPCR ratio results are based on the implicit assumption that only primary predation of intact organisms was detected. Secondary predation, i.e. detection of *P. pouchetii* or *S. marinoi* in the gut content of organisms secondarily consumed by *Calanus* copepods, cannot be distinguished from direct predation using the qPCR method reported here due the high sensitivity of PCR (Harwood et al. 2001). It is therefore possible that the qPCR signals for *P. pouchetii* or *S. marinoi* generated from copepod samples were the result of copepod consumption of microzooplankton, e.g. dinoflagellates or ciliates, that had recently consumed these phytoplankton (see above). Controlled studies of the PCR-detectability of secondary predation in aphid–spider–carabid trophic chains, however, indicate that this trophic pathway generates only weak signals of short duration (Harwood et al. 2001, Sheppard et al. 2005). Furthermore, indirect consumption of naked environmental DNA (eDNA) from *P. pouchetii* or *S. marinoi* by mesocosm-incubated copepods was not controlled for in this experiment. As eDNA likely exists in the dissolved state in seawater and can be rapidly hydrolyzed by marine prokaryotes (Paul et al. 1987), its consumption by particle-feeding *Calanus* is unlikely. The seawater samples filtered for qPCR quantification of *P. pouchetii* and *S. marinoi* were not pre-treated with DNase enzyme to remove eDNA prior to DNA extraction, however the filters utilized for seawater filtration have low binding efficiency for biomolecules including DNA (Pall Corporation, product information). We are therefore confident that the qPCR signals from copepod consumption or from seawater filtration have not been significantly affected by the presence of eDNA in mesocosms or in Raunefjorden.

qPCR results for *P. pouchetii* and *S. marinoi* in copepod samples, and hence qPCR ratios, are based

on pools of 5 *Calanus* copepod individuals per sample. We chose to use pools of individuals in order to increase the probability of qPCR signal detection in the event of low copepod feeding rates on targeted phytoplankton (Nejstgaard et al. 2008). We are aware that variability in grazing between copepod individuals may be misrepresented in pooled samples, however our analysis consisted of 3 replicate pools of 5 copepods per mesocosm per sampling day. The high spread in qPCR signals from replicate copepod samples (Fig. 3A for *P. pouchetii*, Fig. 3D for *S. marinoi*) nevertheless identified clear trends in relative grazing by copepods, and in addition underscores the importance of replication in analysis of copepod diet using molecular analysis.

In spite of some methodological challenges addressed above, we have been able to show that the use of taxon-specific qPCR ratios to trace relative grazing by copepods on mixed assemblages of microbial eukaryotes dominated by either *P. pouchetii* or *S. marinoi* is an informative tool for studying mesozooplankton grazing. Furthermore, our results provide support for previous studies suggesting that *Calanus* copepods exhibit grazing selectivity that is de-coupled from specific prey density and likely based on nutritional content or chemical composition of prey. The complete biological impact of decoupling prey selection from prey abundance driven by life history (bloom development) is complex. However, given that the relative importance (in terms of abundance) of major phytoplankton groups seems to be changing in favor of taxa with low bioavailability as a consequence of global climate change (Moran 2015), such processes may become increasingly important. Further investigation of the full range of copepod prey organisms using universal molecular methods is therefore necessary to increase our understanding of copepod feeding selection and the efficiency of the marine microbial food web.

**Acknowledgments.** This study was funded by the Research Council of Norway (RCN) research project 'A novel cross-disciplinary approach to solve an old enigma: the food-web transfer of the mass-blooming phytoplankton *Phaeocystis pouchetii*' (Phaeonigma, project number 204479/F20). Additional support was received from the European Research Council Advanced Grant ERC-AG-LS8 'Microbial Network Organisation' (MINOS, project number 250254), the RCN project 'Processes and players in Arctic marine pelagic food webs — biogeochemistry, environment and climate change' (MicroPolar, project number 225956/E10) and from the VELUX Foundation Grant # VKR022608.

## LITERATURE CITED

- Barofsky A, Simonelli P, Vidoudez C, Troedsson C, Nejstgaard JC, Jakobsen HH, Pohnert G (2010) Growth phase of the diatom *Skeletonema marinoi* influences the metabolic profile of the cells and the selective feeding of the copepod *Calanus* spp. *J Plankton Res* 32:263–272
- Calbet A, Sazhin AF, Nejstgaard JC, Berger SA and others (2014) Future climate scenarios for a coastal productive planktonic food web resulting in microplankton phenology changes and decreased trophic transfer efficiency. *PLoS ONE* 9:e94388
- Cleary AC, Durbin EG, Rynearson TA (2012) Krill feeding on sediment in the Gulf of Maine (North Atlantic). *Mar Ecol Prog Ser* 455:157–172
- Durbin EG, Casas MC, Rynearson TA, Smith DC (2008) Measurement of copepod predation on nauplii using qPCR of the cytochrome oxidase I gene. *Mar Biol* 153: 699–707
- Durbin EG, Casas MC, Rynearson TA (2012) Copepod feeding and digestion rates using prey DNA and qPCR. *J Plankton Res* 34:72–82
- Dutz J, Breteler WK, Kramer G (2005) Inhibition of copepod feeding by exudates and transparent exopolymer particles (TEP) derived from a *Phaeocystis globosa* dominated phytoplankton community. *Harmful Algae* 4:929–940
- Estep KW, Nejstgaard JC, Skjoldal HR, Rey F (1990) Predation by copepods upon natural populations of *Phaeocystis pouchetii* as a function of the physiological state of the prey. *Mar Ecol Prog Ser* 67:235–249
- Fessenden L, Cowles TJ (1994) Copepod predation on phagotrophic ciliates in Oregon coastal waters. *Mar Ecol Prog Ser* 107:103–111
- Frischer ME, Danforth JM, Tyner LC, Leverone JR, Marelli DC, Arnold WS, Blake NJ (2000) Development of an Argopecten-specific 18S rRNA targeted genetic probe. *Mar Biotechnol* 2:11–20
- Gasparini S, Daro MH, Antajan E, Tackx M, Rousseau V, Parent JY, Lancelot C (2000) Mesozooplankton grazing during the *Phaeocystis globosa* bloom in the southern bight of the North Sea. *J Sea Res* 43:345–356
- Gibson UE, Heid CA, Williams PM (1996) A novel method for real time quantitative RT-PCR. *Genome Res* 6: 995–1001
- Gifford DJ, Dagg MJ (1988) Feeding of the estuarine copepod *Acartia tonsa* Dana: carnivory vs. herbivory in natural microplankton assemblages. *Bull Mar Sci* 43:458–468
- Goncalves RJ, Kiørboe T (2015) Perceiving the algae: how feeding-current copepods detect their nonmotile prey. *Limnol Oceanogr* 60:1286–1297
- Hansen FC (1995) Trophic interactions between zooplankton and *Phaeocystis* cf. *globosa*. *Helgol Meeresunters* 49: 283–293
- Hansen FC, Van Boekel WHM (1991) Grazing pressure of the calanoid copepod *Temora longicornis* on a *Phaeocystis* dominated spring bloom in a Dutch tidal inlet. *Mar Ecol Prog Ser* 78:123–129
- Harwood JD, Phillips SW, Sunderland KD, Symondson WOC (2001) Secondary predation: quantification of food chain errors in an aphid-spider-carabid system using monoclonal antibodies. *Mol Ecol* 10:2049–2057
- Holm-Hansen O, Riemann B (1978) Chlorophyll a determination: improvements in methodology. *Oikos* 30:438–447
- Huntley M, Tande K, Eilertsen HC (1987) On the trophic fate

- of *Phaeocystis pouchetii* (Hariot). II. Grazing rates of *Calanus hyperboreus* (Krøyer) on diatoms and different size categories of *Phaeocystis pouchetii*. J Exp Mar Biol Ecol 110:197–212
- Huo YZ, Wang SW, Sun S, Li CL, Liu MT (2008) Feeding and egg production of the planktonic copepod *Calanus sinicus* in spring and autumn in the Yellow Sea, China. J Plankton Res 30:723–734
- Irigoin X, Flynn KJ, Harris RP (2005) Phytoplankton blooms: a 'loophole' in microzooplankton grazing impact? J Plankton Res 27:313–321
- Jacobsen A, Egge JK, Heimdal BR (1995) Effects of increased concentration of nitrate and phosphate during a springbloom experiment in mesocosm. J Exp Mar Biol Ecol 187:239–251
- Jakobsen HH, Tang KW (2002) Effects of protozoan grazing on colony formation in *Phaeocystis globosa* (Prymnesiophyceae) and the potential costs and benefits. Aquat Microb Ecol 27:261–273
- Jakobsen HH, Halvorsen E, Hansen BW, Visser AW (2005) The effects of food concentrations on prey motility on feeding *Acartia tonsa* and *Temora longicornis*: the importance of feeding modes. J Plankton Res 27:775–785
- Jónasdóttir SH, Visser AW, Richardson K, Heath MR (2015) Seasonal copepod lipid pump promotes carbon sequestration in the deep North Atlantic. Proc Natl Acad Sci USA 112:12122–12126
- Jonsson PR, Tiselius P (1990) Feeding behaviour, prey detection and capture efficiency of copepod *Acartia tonsa* feeding on planktonic ciliates. Mar Ecol Prog Ser 60: 35–44
- Kjørboe T, Nielsen TG (1994) Regulation of zooplankton biomass and production in a temperate coastal ecosystem. I. Copepods. Limnol Oceanogr 39:493–507
- Kjørboe T, Visser AW (1999) Predation and prey perception in copepods due to hydromechanical signals. Mar Ecol Prog Ser 179:81–95
- Kjørboe T, Saiz E, Viitasalo M (1996) Prey switching behaviour in the planktonic copepod *Acartia tonsa*. Mar Ecol Prog Ser 143:65–75
- Klein Breteler WCM, Koski M (2003) Development and grazing of *Temora longicornis* (Copepoda, Calanoida) nauplii during nutrient limited *Phaeocystis globosa* blooms in mesocosms. Hydrobiologia 491:185–192
- Kleppel GS (1993) On the diets of calanoid copepods. Mar Ecol Prog Ser 99:183–195
- Kleppel GS, Holliday DV, Pieper RE (1991) Trophic interactions between copepods and microplankton: a question about the role of diatoms. Limnol Oceanogr 36:172–178
- Koski M, Dutz J, Breteler WK (2005) Selective grazing of *Temora longicornis* in different stages of a *Phaeocystis globosa* bloom—a mesocosm study. Harmful Algae 4: 915–927
- Kuhlisch C, Pohnert G (2015) Metabolomics in chemical ecology. Nat Prod Rep 32:937–955
- Leising AW, Horner R, Pierson JJ, Postel J, Halsband-Lenk C (2005a) The balance between microzooplankton grazing and phytoplankton growth in a highly productive estuarine fjord. Prog Oceanogr 67:366–383
- Leising AW, Pierson JJ, Halsband-Lenk C, Horner R, Postel J (2005b) Copepod grazing during spring blooms: can *Pseudocalanus newmani* induce trophic cascades? Prog Oceanogr 67:406–421
- Mayzaud P, Razouls S (1992) Degradation of gut pigment during feeding by a subantarctic copepod: importance of feeding history and digestive acclimation. Limnol Oceanogr 37:393–404
- Moran M A (2015) The global ocean microbiome. Science 350:aac8455
- Nejstgaard JC, Gismervik I, Solberg PT (1997) Feeding and reproduction by *Calanus finmarchicus*, and microzooplankton grazing during mesocosm blooms of diatoms and the coccolithophore *Emiliania huxleyi*. Mar Ecol Prog Ser 147:197–217
- Nejstgaard JC, Hygum BH, Naustvoll LJ, Båmstedt U (2001) Zooplankton growth, diet and reproductive success compared in simultaneous diatom- and flagellate-microzooplankton-dominated plankton blooms. Mar Ecol Prog Ser 221:77–91
- Nejstgaard JC, Frischer ME, Verity PG, Anderson JT and others (2006) Plankton development and trophic transfer in seawater enclosures with nutrients and *Phaeocystis pouchetii* added. Mar Ecol Prog Ser 321:99–121
- Nejstgaard JC, Tang KW, Steinke M, Dutz J, Koski M, Antajan E, Long JD (2007) Zooplankton grazing on *Phaeocystis*: a quantitative review and future challenges. Biogeochemistry 83:147–172
- Nejstgaard JC, Frischer ME, Simonelli P, Troedsson C and others (2008) Quantitative PCR to estimate copepod feeding. Mar Biol 153:565–577
- Paul JH, Jeffrey WH, DeFlaun MF (1987) Dynamics of extracellular DNA in the marine environment. Appl Environ Microbiol 53:170–179
- Peterson CG, Jones TL (2003) Diatom viability in insect fecal material: comparison between two species, *Achnanthes lanceolatum* and *Synedra ulna*. Hydrobiologia 501: 93–99
- Pohlert T (2015) PMCMR: Calculate pairwise multiple comparisons of mean rank sums. R package version 1.1. <https://CRAN.R-project.org/package=PMCMR>
- R Core Team (2015) R: a language and environment for statistical computing. R Foundation for Statistical Computing, Vienna. [www.r-project.org](http://www.r-project.org)
- Schoemann V, Becquevort S, Stefels J, Rousseau V, Lancelot C (2005) *Phaeocystis* blooms in the global ocean and their controlling mechanisms: a review. J Sea Res 53: 43–66
- Sheppard SK, Bell J, Sunderland KD, Fenlon J, Skervin D, Symondson WOC (2005) Detection of secondary predation by PCR analyses of the gut contents of invertebrate generalist predators. Mol Ecol 14:4461–4468
- Sherr EB, Sherr BF (2007) Heterotrophic dinoflagellates: a significant component of microzooplankton biomass and major grazers of diatoms in the sea. Mar Ecol Prog Ser 352:187–197
- Simonelli P, Troedsson C, Nejstgaard JC, Zech K, Larsen JB, Frischer ME (2009) Evaluation of DNA extraction and handling procedures for PCR-based copepod feeding studies. J Plankton Res 31:1465–1474
- Sommer F, Stibor H, Sommer U, Velimirov B (2000) Grazing by mesozooplankton from Kiel Bight, Baltic Sea, on different sized algae and natural seston size fractions. Mar Ecol Prog Ser 199:43–53
- Stelfox-Widdicombe CE, Archer SD, Burkill PH, Stefels J (2004) Microzooplankton grazing in *Phaeocystis* and diatom-dominated waters in the southern North Sea in spring. J Sea Res 51:37–51
- Stoecker DK, Capuzzo JM (1990) Predation on protozoa: its

- importance to zooplankton. *J Plankton Res* 12:891–908
- Stoecker DK, Nejstgaard JC, Madhusoodhanan R, Pohnert F and others (2015) Underestimation of microzooplankton grazing in dilution experiments due to inhibition of phytoplankton growth. *Limnol Oceanogr* 60:1426–1438
  - Sullivan LJ (2010) Gut evacuation of larval *Mnemiopsis leidyi* A. Agassiz (Ctenophora, Lobata). *J Plankton Res* 32:69–74
  - Thingstad TF, Bellerby RGJ, Bratbak G, Børsheim KY and others (2008) Counterintuitive carbon-to-nutrient coupling in an Arctic pelagic ecosystem. *Nature* 455:387–390
  - Troedsson C, Frischer ME, Nejstgaard JC, Thompson EM (2007) Molecular quantification of differential ingestion and particle trapping rates by the appendicularian *Oikopleura dioica* as a function of prey size and shape. *Limnol Oceanogr* 52:416–427
  - Troedsson C, Simonelli P, Nägele V, Nejstgaard JC, Frischer ME (2009) Quantification of copepod gut content by differential length amplification quantitative PCR (dla-qPCR). *Mar Biol* 156:253–259
  - Wickham H (2009) *ggplot2: Elegant graphics for data analysis*. Springer, New York, NY

*Editorial responsibility: Edward Durbin,  
Narragansett, Rhode Island, USA*

*Submitted: June 2, 2015; Accepted: November 17, 2015  
Proofs received from author(s): January 11, 2016*